

## Direct binding of Talin to Rap1 is required for Cell-ECM adhesion in *Drosophila*

Camp D<sup>1</sup>, Haage A<sup>1</sup>, Solianova V<sup>1</sup>, Castle WM<sup>2</sup>, Xu QA<sup>1</sup>, Lostchuck E<sup>1</sup>, Goult BT<sup>2</sup> and Tanentzapf G.<sup>1\*</sup>

1. Department of Cellular and Physiological Sciences, University of British Columbia, Vancouver, Canada, V6T 1Z3
2. School of Biosciences, University of Kent, Canterbury CT2 7NJ, UK.

\* Author for correspondence:

**Guy Tanentzapf**

Life Sciences Centre

2350 Health Science Mall

Vancouver, BC

V6T 1Z3

Phone: 604-827-4334

Email: [tanentz@mail.ubc.ca](mailto:tanentz@mail.ubc.ca)

## Abstract

Attachment of cells to the Extracellular Matrix (ECM) via integrins is essential for animal development and tissue maintenance. The cytoplasmic protein Talin is necessary for linking integrins to the cytoskeleton and its recruitment is a key step in the assembly of the adhesion complex. However, the mechanisms that regulate Talin recruitment to sites of adhesion *in vivo* are still not well understood. Here we show that Talin recruitment to, and maintenance at, sites of integrin-mediated adhesion requires a direct interaction between Talin and the GTPase Rap1. A mutation that blocks the direct binding of Talin to Rap1 abolished Talin recruitment to sites of adhesion and the resulting phenotype phenocopies null alleles of Talin. Moreover, we show that Rap1 activity modulates Talin recruitment to sites of adhesion via its direct binding to Talin. These results identify the direct Talin-Rap1 interaction as a key *in vivo* mechanism for controlling integrin-mediated cell-ECM adhesion.

## Introduction

The assembly and maintenance of tissue architecture is dependent on large multiprotein cell adhesion complexes. This presents a challenge to cells as they need to coordinate the delivery of a large number of diverse proteins to specific sites at the cell membrane. Importantly, the process of recruiting components of the complex to nascent sites of adhesion and assembling them into a functional unit provides a valuable opportunity for regulating cell adhesion. For these reasons, there has been a great deal of interest in understanding the mechanisms that control recruitment and delivery of adhesion complex components to the cell cortex. In the case of integrin-mediated cell-ECM adhesion, protein recruitment to the cell cortex is regulated by mechanisms that involve trafficking machinery and modulation of protein-protein interactions within the complex (Paul et al., 2015; Wehrle-Haller, 2012). In recent years evidence has accumulated from *in vivo* studies that the regulation of integrin adhesion complex dynamics is important during tissue development and maintenance (Costa and Parsons, 2010; Daley and Yamada, 2013; Wolfenson et al., 2013). Consequently, the use of mutations that alter the strength and stability of integrin adhesions provide a valuable opportunity to interrogate the role of cell-ECM attachment for a wide array of developmental processes.

The protein Talin is a central component of the integrin adhesion complex and is essential for the assembly and maintenance of integrin-based cell-ECM attachment (Klapholz and Brown, 2017). Talin binds to the  $\beta$ -integrin cytoplasmic tail directly and then links integrins to the cytoskeleton either directly, through its actin binding domains (Franco-Cea et al., 2010) or indirectly, by recruiting downstream components of the adhesion complex (Giannone et al., 2003; Tanentzapf et al., 2006). In addition, Talin plays an important role in regulating the affinity of integrins for their ECM ligands through regulating integrin activation (Shattil et al., 2010; Tadokoro et al., 2003). Talin contains two known integrin-binding sites (IBSs): IBS-1 is located in the N-terminal end of the protein, while IBS-2 is in the C-terminus. The IBS-1 domain of Talin, also known as the Talin head domain, has been extensively implicated in integrin activation. Expression of IBS-1 is sufficient to activate integrins in diverse contexts (Calderwood et al., 1999; Ellis et al., 2011). It is thought that the binding of the Talin IBS-1 to the  $\beta$ -integrin cytoplasmic tail causes a change in the tail's angle relative to the plasma membrane, disrupting interactions between the tails of  $\alpha$  and  $\beta$  integrin and inducing integrin activation (Wegener et al., 2007). The mechanisms that control the recruitment of Talin to sites of adhesion at the cell cortex are therefore important for the regulation of integrin function (Calderwood et al., 2013; Klapholz and Brown, 2017).

Another important, and well characterized, protein that regulates integrin function is the small GTPase Rap1. Rap1 is known to be an activator of integrin function in diverse biological contexts (Boettner and Van Aelst, 2009). Currently, Rap1-mediated integrin activation is thought to occur via a complex made up of Rap1, the Rap1 effector RIAM (Rap1-GTTP-interacting adaptor molecule), and Talin. RIAM is an adapter molecule whose main function has been proposed to be the targeting of Talin to integrins (Han et al., 2006). Rap1 binds directly to RIAM through its Ras-association domain and RIAM binds to Talin through 30 residues at its N-terminal. The complex is recruited to the cell cortex through a membrane targeting sequence in Rap1. Intriguingly, a construct containing only a fusion of the membrane targeting sequence of Rap1 and the Talin binding sequence of RIAM is fully sufficient to

recruit Talin to the membrane and induce integrin activation (Lee et al., 2009). Nonetheless, recent evidence has suggested that in many contexts RIAM is dispensable for Talin recruitment to sites of adhesion (Stritt et al., 2015). This raises the possibility that the ability of Rap1 to regulate integrin activity through Talin might also work via an alternative mechanism. More recently, evidence has emerged that Rap1 can bind Talin directly and regulate its recruitment to the membrane. Biochemical experiments already have shown weak direct binding between Talin and Rap1, and suggested this interaction can serve as a mechanism for targeting Talin to the membrane (Goult et al., 2010; Zhu et al., 2017). Furthermore, in the slime mold *Dictyostelium*, direct binding of Rap1 to Talin was shown to be necessary for adhesion during multicellular development (Plak et al., 2016). However, whether the direct binding of Rap1 to Talin is relevant in complex multicellular organisms, and if so in what contexts, has not been established.

*Drosophila* serves as a powerful model system for studying the function of components of the integrin adhesion complex. In particular, the fly has proven to be useful for *in vivo* structure-function analysis of components of the integrin adhesion complex. Loss-of-function mutations in *mysospheroid* (*mys*), the gene that encodes the main  $\beta$ -integrin subunit in flies, cause severe embryonic defects in multiple tissues (Leptin et al., 1989). Among the best-characterized integrin dependent processes in the fly is the stable attachment of muscle cells to tendon cells through the ECM in prominent integrin-based adhesions at myotendinous junctions (MTJs) (Schweitzer et al., 2010). Additionally, two dynamic integrin-adhesion based morphogenetic processes, Germband Retraction (GBR) and the wound closure-like process of Dorsal Closure (DC), have been analyzed in detail (Narasimha and Brown, 2004; Schöck and Perrimon, 2003). Forward genetics screens in the fly have led to the isolation and characterization of mutations in more than a dozen genes that encode cytoplasmic factors involved in integrin function, including, Pinch (Clark et al., 2003), Paxillin (Yagi et al., 2001), Tensin (Torgler et al., 2004), ILK (Zervas et al., 2001), and Talin (Brown et al., 2002). *Drosophila* Talin is particularly important for integrin-mediated adhesion in flies. Flies lacking Talin exhibit a phenotype that is largely indistinguishable from that observed following loss of integrins. In Talin mutants, muscle attachment to tendon cells fails, and both GBR and DC are disrupted (Brown et al., 2002). The fly has proven to be a particularly useful system in which to analyze Talin function and detailed structure-function analysis of specific domains of Talin has provided mechanistic insight into its regulation during tissue development and homeostasis (Ellis et al., 2011; Ellis et al., 2013; Franco-Cea et al., 2010; Tanentzapf and Brown, 2006).

Here, we have characterized the role of direct binding of Talin to Rap1 *in vivo*. Using a CRISPR/Cas9-based strategy, we introduced a point mutation that specifically blocks the direct binding of Talin to Rap1 into genomic Talin in *Drosophila*. We find that disrupting the ability of Talin to directly bind Rap1 completely abolished its function. In these mutants, Talin was not recruited to sites of adhesion and comprehensive phenotypic analysis confirmed that the resulting phenotype was very similar to that seen in Talin null flies. Furthermore, using Talin and Rap1 transgenes, we provide evidence showing that Rap1 activity regulates Talin recruitment to the membrane via their direct interaction. This work establishes that direct binding of Talin and Rap1 regulates Talin recruitment to sites of adhesion and is thus an essential regulator of adhesion complex assembly and maintenance *in vivo*.

## Results

### Direct binding of the Talin F0 domain to Rap1 is conserved in flies.

Several studies have defined a region in Talin that binds directly to Rap1 (Goult et al., 2010; Plak et al., 2016; Zhu et al., 2017). The Talin head domain is composed of four subdomains labelled F0, F1, F2, and F3 with F1–F3 making up the FERM (4.1/ezrin/radixin/moesin)-like domain (Fig. 1A). The site of interaction between Rap1 and Talin lies in the F0 domain. This region is required for integrin activation (Bouaouina et al., 2008) and is well conserved between fly and vertebrate Talin (Fig. 1B). Homology modelling showed that the binding interfaces of fly Rap1 and the Talin F0 domain are very similar to those shown to be important in the recently solved structure of vertebrate Talin bound to Rap1b (PDB ID 6ba6, Zhu et al., 2017). Notably, positively charged surface residues found in Rap1-binding domains are conserved in fly Talin (Fig. 1B-D, Goult et al., 2010). NMR experiments using <sup>15</sup>N-labelled fly Talin F0 and Rap1b showed clear chemical shift changes when Rap1b was added to Talin F0 indicating a direct interaction (Fig. 1E). To further analyse this chemical shift data, we used a <sup>13</sup>C-<sup>15</sup>N-labeled F0 domain (residues 1–87) to complete the backbone assignment of Talin F0. The weighted <sup>1</sup>H, <sup>15</sup>N chemical shifts in F0 induced by Rap1b (Fig. 1E) were plotted as a function of residue number (Supplementary Fig. 1) and plotted onto the structure of the F0:Rap1b complex (Fig. 1C-D). From this NMR and structural data it was shown that a conserved lysine residue (K15 in vertebrate Talin, K17 in fly Talin) was crucial for binding of Rap1 to the Talin F0 (Fig. 1B, Goult et al., 2010; Zhu et al., 2017). We introduced the equivalent K17E mutation into the fly Talin F0 and found that it did not affect the folding of the protein (Supplementary Fig. 1). Importantly, NMR experiments confirmed that the K17E mutation in fly Talin completely abrogated F0 binding to Rap1 (Fig. 1F and Supplementary Fig. 2). These results suggest that the direct binding of Talin to Rap1 through the Talin F0 domain is evolutionarily conserved and identifies K17E as an effective tool to disrupt this binding.

### Generation of a Talin mutant that blocks the direct binding of the Talin F0 domain to Rap1.

Next, we introduced the K17E mutation into *rhea*, the gene that encodes Talin in flies. We utilized CRISPR/Cas9-mediated homology-directed repair (HDR) with a double-stranded DNA (dsDNA) donor template to genetically engineer the endogenous *rhea* locus (Fig. 2). We employed two guide RNAs (gRNAs) targeting sites 5' and 3' of the sequence corresponding to K17, as well as a dsDNA donor with homology arms containing approximately 1kb of sequence flanking the targeted cleavages sites in addition to the targeted point mutation (Fig. 2A). To select for targeted events our donor vector also contained a visible DsRed eye marker flanked by loxP sites for CRE-mediated removal. The residual 34bp loxP site leftover from the CRE recombination was specifically introduced in an area with a low degree of sequence conservation. Furthermore, previous studies showed that even a large 7.5kb Minos insertions (Mi{ET1}MB11781) had no noticeable effects on Talin function at this site (Fig. 2A, Bellen et al., 2004). Using this approach, we isolated a number of mutant lines. These were sequenced extensively both upstream and downstream of the K17E mutation site to confirm the presence of the mutation and to ensure no other deleterious events took place at the *rhea* locus (Fig. 2B, C). We noted that all the mutant *rhea*<sup>K17E</sup> lines were embryonic lethal. Importantly, the *rhea*<sup>K17E</sup> allele failed to

complement null alleles of *rhea*. Moreover, introducing a ubiquitously expressing Talin rescue construct (*ubi::Talin*, Tanentzapf and Brown, 2006) into the background of null alleles of *rhea* or the *rhea*<sup>K17E</sup> allele rescued the embryonic lethality associated with loss of Talin to the same extent, that is until pupation (Fig. 2D). Taken together these data show that the *rhea*<sup>k17</sup> allele behaves like a genetic loss-of-function null allele of Talin.

### **Blocking the direct binding of Rap1 to Talin through the F0 domain disrupts embryonic tissue morphogenesis.**

To further understand the nature of the phenotypes caused by introducing the K17E mutation in Talin, the embryonic phenotype of the *rhea*<sup>K17E</sup> allele was analyzed in detail. Although loss of Talin impacts diverse embryonic phenotypes, we focused on four integrin-dependent processes that provide a broad overview of integrin-mediated cell-ECM adhesion during development. Specifically, two dynamic morphogenetic processes, dorsal closure (DC) and germband retraction (GBR) were analyzed. In addition, two stable long-term adhesive processes, muscle attachment via the ECM to the epidermis at myotendinous junctions (MTJs), and epithelial adhesion in the fly wing, were also studied.

Large integrin-based adhesions form at MTJs starting mid-way through fly embryogenesis (Fig. 3A, D). Loss of integrins or Talin results in loss of muscle attachment to the tendons at the MTJs and subsequent rounding of the muscles (Leptin et al., 1989, Fig. 3B, E, L). Severe disruption to MTJs, similar to that seen in a null allele of *rhea*, was observed in mutants for the *rhea*<sup>K17E</sup> allele (Fig. 3C, F, L). Another similarity between mutants from the null and *rhea*<sup>K17E</sup> alleles was that the full extent of the mutant phenotypes was observed only once the maternal contribution of wildtype Talin was eliminated via the use of germline clones (see materials and methods), as the maternal contribution provided a substantial amount of phenotypic rescue (Fig. 3G-I, L). The morphogenetic movements of germband retraction (GBR), a coordinated cell movement involving rapid posterior and ventral movement of the germband, and dorsal closure (DC), the closing of a large dorsal hole in the embryo, are both dependent on integrin and Talin (Brown et al., 2002; Narasimha and Brown, 2004; Schöck and Perrimon, 2003). Introducing the K17E mutation strongly disrupted DC and a comparable proportion of the embryos of either the null or the *rhea*<sup>K17E</sup> genotype failed to complete the process (Fig. 3A-C, K, M). Similar results were obtained for GBR, as a nearly identical proportion of the embryos of either the null or *rhea*<sup>K17E</sup> genotype failed to complete the process (Fig. 3A-C, J, O). As observed for the MTJ phenotype, both DC and GBR were fully rescued in the null and *rhea*<sup>K17E</sup> alleles by the presence of the maternal wildtype Talin (Fig. 3M, O). Finally, the ability of integrin-mediated adhesion to support the attachment of the two layers of epithelial cells that make up the fly wing was assayed by quantifying the proportion of flies with the characteristic wing-blistering defect that is caused by loss of cell-ECM adhesion. In this context, introducing the K17E mutation into Talin resulted in wing blistering in a similar proportion of flies to that seen with a null allele of Talin (Fig. 3P). Taken together these data show that, at least in the context of tissue level phenotypes, introducing the K17E mutation into Talin abolishes its function to a similar extent as complete loss-of-function mutations in Talin.

### **Blocking the direct binding of Rap1 to Talin through the F0 domain disrupts the assembly of the integrin adhesion complex.**

The strong functional defects caused by the K17E mutation during fly development suggested a severe disruption to integrin-mediated adhesion. Such a defect could be caused by problems with the assembly of the adhesions. To analyze adhesion complex assembly in detail, we employed a method to study co-localization of integrins with markers for the integrin adhesion complex (Ellis et al., 2011; Ellis et al., 2013; Ellis et al., 2014). Specifically, the distribution of Integrin (Leptin et al., 1989), Paxillin (Yagi et al., 2001) and PINCH (Clark et al., 2003) was used to visualize the integrin adhesion complex in wildtype and mutant embryos (Fig. 4). In wildtype MTJs, both Paxillin and PINCH concentrated at the MTJs and their distribution largely overlapped with that of integrin (Fig. 4A, G and D, J, respectively). In contrast, in embryos lacking Talin, integrin still localized to MTJs though at much lower levels than the wildtype, but both Paxillin and PINCH failed to concentrate at the MTJs (Fig. 4B, H and E, K, respectively). Similarly, mutant *rhea*<sup>K17E</sup> embryos localized integrin weakly to MTJs, but both Paxillin and PINCH failed to concentrate at the MTJs (Fig. 4C, I and F, L, respectively). These results suggest Talin containing the K17E mutation was unable to support the assembly of the integrin adhesion complex.

### **Blocking the direct binding of Rap1 to Talin through the F0 domain affects Talin localization to the cell-cortex.**

The strong loss-of-function phenotypes and the failure to assemble the integrin adhesion complex produced by the K17E mutation could result from changes in the production or localization of Talin. Analysis using qPCR showed no statistically significant differences in levels of transcription of Talin RNA from either the wildtype or the engineered *rhea*<sup>K17E</sup> loci (Fig. 5A). Furthermore, western blots showed no statistically significant differences in the overall levels of Talin protein in the wildtype or the *rhea*<sup>K17E</sup> embryos (Fig. 5B, C). To analyze the relative stability of Talin with the K17E mutation at sites of adhesion in comparison to the wildtype version of the protein, transgenes were used that contained a ubiquitously expressed full-length Talin construct that was either wildtype (ubi-talinGFP-WT, Tanentzapf and Brown, 2006) or contained the K17E mutation (ubi-talinGFP\*K17E). Fluorescence recovery after photobleaching (FRAP) experiments were carried out with ubi-talinGFP-WT and ubi-talinGFP\*K17E, in a background that also contained the wildtype untagged genomic Talin. These FRAP experiments showed a substantially higher mobile fraction of Talin containing the K17E mutation, consistent with reduced stability of the K17E mutant Talin at sites of adhesion (Fig. 5K).

Consistent with this result, there was a dramatic reduction of Talin at MTJs in *rhea*<sup>K17E</sup> embryos compared to wildtype (Fig. 5D-J). In wildtype MTJs, integrin and Talin co-localize and appear as a discrete line at muscle attachments (Fig. 5G, J). In mutant embryos of either the null and *rhea*<sup>K17E</sup> alleles, integrin was present at MTJs although at notably lower levels compared to wildtype, Talin was not detected in the MTJs (Fig. 5H-J). To account for the possibility that the defects in MTJ architecture in null or *rhea*<sup>K17E</sup> mutant embryos underlie this recruitment phenotype, we analyzed Talin recruitment in the background of maternally rescued and heterozygous mutant embryos, which both have intact MTJs (Fig. 5L-Q). In embryos containing one mutant copy of either a null or a *rhea*<sup>K17E</sup> mutant allele a similar reduction in the levels of Talin at MTJs was observed compared to the wildtype (Fig. 5L-N, Q). Furthermore, in maternally rescued null or *rhea*<sup>K17E</sup> mutant embryos a substantial and

comparable reduction in the levels of Talin at MTJs was observed compared to the wildtype (Fig. 5O-Q). Similar localization defects were observed in other tissues, for example mutant clones of either the null or the *rhea*<sup>K17E</sup> allele in fly wing discs showed no detectable levels of Talin at the cell cortex, where Talin is usually found (Fig. 5R-T). Taken together these results show that although Talin containing the K17E mutation is transcribed and translated, it is not properly recruited to or maintained at the cell cortex.

### **Talin-head recruitment to sites of adhesion is regulated by Rap1 through binding to the F0 domain.**

Based on the effects of the K17E mutation on Talin localization we hypothesized that the direct binding between Rap1 and the F0 domain of the Talin head plays an important role in regulating the recruitment and/or maintenance of Talin at sites of adhesion. We previously showed that a construct containing the entire Talin head domain (F0, F1, F2, and F3), fused to GFP (TalinHead::GFP), localized efficiently to sites of adhesion at MTJs and was enriched about 3-fold at the MTJs compared to the background staining (Fig. 6A, G, Tanentzapf and Brown, 2006; Tanentzapf et al., 2006). As in previous studies, TalinHead::GFP was also observed in the nucleus, which our past work showed was not a functionally significant localization, but rather an artifact of overexpression of the GFP tagged fusion protein (Ellis et al., 2011; Tanentzapf et al., 2006). Co-expression of a dominant negative version of Rap1 (see materials and methods, Ellis et al., 2013) reduced the localization of TalinHead::GFP in MTJs to near background levels (Fig. 6B, G). In contrast, co-expression of a constitutively active version of Rap1 (see materials and methods, Ellis et al., 2013) enhanced the recruitment of TalinHead::GFP to MTJs by nearly a factor of 4 compared to background staining (Fig. 6C, G). In comparison to these results, a construct containing a fusion of GFP with the F2 and F3 domains of the Talin head (F2F3::GFP), that contains the integrin binding site, but lacks the Rap1 binding F0 domain, localized poorly to MTJs and was enriched by a factor of only about 1.7 compared to background staining at the MTJs (Fig. 6D, H). Importantly, co-expression of either a dominant negative or a constitutively active version of Rap1 did not change the recruitment of F2F3::GFP (Fig. 6E, F, H), in line with what would be expected of a construct that lacks the direct binding site between Talin and Rap1. These experiments suggest that in the context of the Talin head domain, the direct binding to Rap1 plays an important function in its recruitment and/or maintenance at sites of adhesion.

### **Full-length Talin recruitment to sites of adhesion is regulated by Rap1 through binding to the F0 domain.**

Next, the ability of Rap1 to recruit full-length wildtype and K17E mutant Talin was analyzed. Since embryos expressing only the K17E mutant Talin exhibit severe muscle defects that could interfere with the interpretation of the data, these experiments were done using zygotic *rhea*<sup>K17E</sup> mutants, where the embryos still express some maternally provided wildtype Talin during early embryogenesis. This prevents a muscle phenotype from developing until late embryogenesis (see materials and methods, Tanentzapf and Brown, 2006). In wildtype embryos, enrichment of full length Talin was observed at sites of integrin-mediated adhesion at MTJs (Fig. 6I, O). Expression of a dominant negative version of Rap1 (see materials and methods, Ellis et al., 2013) reduced the localization of full-length wildtype Talin at MTJs by

approximately 27% (Fig. 6J, O). In contrast, expression of a constitutively active version of Rap1 (see materials and methods, Ellis et al., 2013) enhanced the recruitment of full-length wildtype Talin to MTJs by approximately 25% compared to background staining (Fig. 6K, O). In zygotic *rhea*<sup>K17E</sup> mutants, a small amount of Talin was recruited to MTJs, which could represent the maternally provided component of Talin in these embryos (Fig. 6L, P). Expression of a dominant negative version of Rap1 slightly reduced the levels of Talin present at the MTJs, in line with the hypothesis that the protein we were detecting was the residual maternally provided Talin (Fig. 6M, P). Importantly, expression of the constitutively active version of Rap1 did not change the levels of Talin detected at the MTJs of zygotic *rhea*<sup>K17E</sup> mutants. This would be the expected outcome if additional recruitment of Talin to sites of adhesion required the direct binding of Rap1 to Talin, as the majority of the Talin present during late embryogenesis in *rhea*<sup>K17E</sup> mutant embryos is the zygotically transcribed Talin K17E protein that cannot bind Rap1 directly (Fig. 6N, P). Taken together our data supports the hypothesis that the direct binding of the Talin F0 domain to Rap1 recruits and/or maintains full-length Talin at sites of integrin-based adhesions.

## Discussion

Here we present a biochemical, genetic, and phenotypic analysis of the role of direct binding of the F0 domain of Talin to Rap1 in *Drosophila*. Our work suggests that, at least in the context of the simplified adhesion complex of *Drosophila*, direct binding between Talin and Rap1 is functionally important for many biological processes. The key role played by Rap1 in controlling integrin-mediated adhesion is extensively documented in the literature (Boettner and Van Aelst, 2009; Bos et al., 2003). Our analysis adds a new function to the repertoire, by which Rap1 can regulate cell-ECM adhesion *in vivo*. This mechanism involves an interaction between Rap1 and Talin, which as a direct binding partner of integrin, lies at the heart of the integrin-adhesion complex and provides Rap1 with a powerful, rapid means of controlling adhesion during the life of an organism.

Although Rap1 has been known as a major regulator of integrin-based adhesion for a long time, the idea that it binds to Talin directly is relatively recent. In *Drosophila* Rap1 plays diverse roles, and in particular is an essential regulator of cell-cell adhesion. Flies completely lacking Rap1 die during the first stages of embryonic development and exhibit severe cellular polarity defects that prevent complex tissue development (Knox et al 2000; Choi et al 2013). Importantly, Rap1 has also been previously implicated in regulating cell-ECM adhesion in *Drosophila*, although the mechanisms remain elusive (Shirinian et al 2010; Huelsmann et al 2006; Ellis et al 2013). Initial indications of a possible direct binding of Talin and Rap1 came from solving the structure of the vertebrate Talin F0 domain, which revealed that the F0 domain exhibited structural homology to the Ras-binding site in RalGDS (Goult et al., 2010). Subsequent studies carried out in both *Dictyostelium* and mammalian cell culture confirmed this direct binding and showed that it is functionally important (Plak et al., 2016; Zhu et al., 2017). Two key functional observations have emerged from these studies: first, the binding of Talin to Rap1 is low affinity and second the binding of Talin to Rap1 regulates Talin recruitment to the membrane (Plak et al., 2016; Zhu et al., 2017). Our work confirms and builds upon these previous observations. The phenotype observed when we introduce a mutation in Talin that

blocks Rap1 binding is indistinguishable from that observed in a null mutation that completely abolishes Talin function. Our FRAP and localization studies suggests that the strong phenotype caused by loss of direct binding of Talin to Rap1 can be explained by a disruption in the ability of the mutant Talin to be localized to and/or be maintained at sites of integrin-mediated adhesion. This result is somewhat surprising because Talin has multiple means of localizing to sites of integrin-mediated adhesion, including two integrin-binding sites, a binding site for the RAP1-binding scaffolding protein RIAM, PIP2 interaction domain, as well as multiple other interaction domains with other components of the adhesion complex (Klapholz and Brown, 2017). It thus appears that, at least in certain contexts, the interaction with Rap1, although weak in nature, is of particular importance for controlling Talin localization. Previous work suggested that the direct interaction between Talin and Rap1 becomes strong when Rap1 was anchored to the membrane (Zhu et al., 2017). In this model Rap1 localization to sites of adhesion creates a microenvironment that favors the recruitment and/or maintenance of Talin (Zhu et al., 2017). This model is very compatible with our findings and helps explain earlier results that defined a role for Rap1 in regulating integrin-mediated adhesion in flies (Shirinian et al 2010; Huelsmann et al 2006; Ellis et al 2013).

The direct binding of Rap1 to Talin also fits very well with our earlier work on Talin autoinhibition (Ellis et al., 2013). We previously showed that Talin that is unable to undergo autoinhibition localizes to the membrane independently of the presence of RIAM (Ellis et al., 2013). This suggested the existence of a RIAM independent mechanism for Talin localization. Intriguingly, previous studies show that the F2F3 domain of Talin contains a conserved RIAM binding site (Yang et al., 2014). Our result show that while the F2F3 domain of Talin localizes to sites of adhesion, it does so less efficiently than the full Talin head domain (containing F0-F3). Furthermore, in contrast to the full-length Talin head construct, the recruitment of a construct containing only the F2F3 domain was not efficiently modulated by the presence of constitutively activated Rap1. This indicates that the main way Rap1 controls the recruitment of the Talin head domain to sites of integrin-mediated adhesion is through direct binding to Talin rather than indirect binding through RIAM. Support for these conclusions comes from studies in mice that showed RIAM was dispensable in most tissues for Talin localization and integrin activation (Stritt et al., 2015). Therefore, it appears that in flies, and possibly, in some tissues in mice, the direct interaction of Talin with Rap is both necessary and sufficient for recruitment and/or maintenance of Talin at sites of integrin-mediated adhesion and that this applies to both autoinhibited and non-autoinhibited Talin.

Our data suggests that a Talin mutant that is unable to bind directly to Rap1 is transcribed, translated, and folds normally, but is unable to function. While we favor a model wherein the strong phenotype we observe is due to an inability to localize and/or maintain Talin at sites of adhesion, we cannot discount several other alternative hypotheses. For example, it could be that, in addition to disrupting the interaction of Talin with Rap1, the K17 mutation also disrupts the interaction of Talin with proteins other than Rap1. Possible candidates for such additional interactions with the Talin F0 domain are other Ras GTPases encoded by the *Drosophila* genome. However, the possible roles of fly GTPases were explored in the context of a genome wide analysis that analyzed, among other phenotypes, disruption to integrin-based myotendinous junctions (Schnorrer et al, 2010). This analysis failed to identify a role

for additional Ras GTPases in integrin-mediated muscle tendon attachment. Additionally, while our experiments show direct F0-Rap1 interactions *in vitro* they do not address the specificity or selectivity of the interaction. The overall weak binding between Talin F0 and Rap1 makes it difficult to illustrate this interaction *in vivo*, which leaves the possibility of indirect binding or that additional, partially redundant, factors are involved. Furthermore, in previous work we showed that making a “headless” version of Talin by deleting the entire Talin head (residues 1–448), while leaving the rest of Talin intact results in a Talin protein that is completely non-functional, but that can still partially localize to sites of adhesion (Ellis et al., 2014). Given this result it is curious that mutating the single K17 residue in the Talin head completely abolishes Talin localization. One possible explanation is that the “headless” version of Talin was expressed from a ubiquitous promoter in an exogenous rescue construct in contrast to the CRISPR approach we used here. Another possible explanation is that the “headless” Talin was tagged with GFP, and was detected using an extremely sensitive GFP specific antibody in contrast to the Talin specific antibody we used to detect the K17 mutant Talin in the present study. Nonetheless, these results hint at the complicated network of positive and negative reinforcement cues that operate on Talin to regulate its localization to the membrane.

It remains to be fully established whether the important role of direct binding between Talin and Rap1 is conserved in vertebrates. The higher complexity of integrin-based adhesions in vertebrates provides alternative regulatory mechanisms that can mask the sort of dramatic phenotypic effects observed in disruptions of the simpler integrin-based adhesions found in the fly. Consistent with this idea is the recent analysis of mice containing a mutation in Talin designed to block the interaction of the F0 domain of Talin with Rap1 (Lagarrigue et al 2018). This work shows that, at least in the context of blood platelets, the direct interaction between the F0 domain and Rap1 is not essential for integrin activation. This suggests two possible differences between the fly and vertebrate integrin-based adhesions, the first is that in vertebrates Talin can be recruited to the membrane by multiple, Rap1 independent, mechanisms and the second is that in vertebrates, Rap1 binds to Talin directly through another interaction that does not involve the F0 domain and which is not conserved in flies. Nonetheless, by showing in the fly that Rap1 binding is essential for Talin recruitment to sites of adhesion our work raises the possibility that, at least in some contexts in vertebrates, the direct binding of Talin to Rap1 may prove to be functionally important.

## Materials and Methods

### Molecular biology

The generation of ubi-talinGFP was previously described (Yuan et al., 2010). To make the pUbi-talinEGFP\*K17E mutant construct, pBS-talinGFP was mutated using the QuikChange Lightning mutagenesis kit (Stratagene). The talinGFP\*K17E cassette was sub-cloned into the pUbi63E vector using a strategy similar to that used to generate the WT talinGFP construct (Yuan et al., 2010). The making of pUASp-GFP-TalinHead, F2F3, UAS Rap1CA, and UAS Rap1 DN was described previously (Tanentzapf et al., 2006, Ellis et al. 2013). The generation of the K17E mutant described here (Fig. 2) is based on a modified version of the following protocols (<http://flycrispr.molbio.wisc.edu> and Gratz et al., 2014). The following target sequence were respectively used for S1 and S2:

GAAACCACCCCAAAGCGCAAGG and GATAAACAGTCCATATTCGCTGG.

The first homology arm was directly amplified from genomic drosophila DNA using the following primers:

GCACACCTGCGATCTCGCCTTGTTTCGGCACATACGAGC and

GATTCACCTGCGCACTTATTACAATTTTGAGCTTATGTTTTTAAGA. The

second arm containing the K17E mutation as well as the second homology arm was amplified from pUBiK17E plasmid using the following primers:

AGGAGCTCTTCATATTAATAATGAGGAAATTCGTTGAAATTT and

ACGTGCTCTTCaGACGTCGCCAAAGTCCAGAGTGA. Both arms were then

seamlessly cloned in the pHD-DsRed (Gratz et al., 2014) respectively, using AarI and SapI sites to generate the double stranded donor DNA. S1 and S2 targeting gRNAs were cloned by annealing the corresponding target sequence oligonucleotides into the pU6-BbsI-chiRNA plasmid (Gratz et al., 2014) via the BbsI restriction sites. The CRISPR injection mix containing the double stranded donor plasmid (500 ng/ $\mu$ L) along with both targeting plasmids (100 ng/ $\mu$ L each) was sent to Bestgene Inc. for injection. K17E transgenic flies were identified by eye color screening using the DsRed gene included in the donor DNA. This visible eye marker was then excised by crossing K17E mutants to P{y[+mDint2]=Crey}1b flies expressing Cre recombinase and leaving behind a residual 34bp residual loxP site. The resulting K17E mutant was then recombined in an FRT2A background and sequenced using standard techniques (Fig. 2D).

### Fly stocks and genetics

Unless otherwise specified all experiments were performed in mutant background such that wild type maternal contributions of Talin were eliminated using the *rhea*<sup>79a</sup> or *rhea*<sup>K17E</sup> alleles and the dominant female sterile technique (Chou and Perrimon, 1996). Females of the genotype yw, hs-Flp/+;; *rhea*<sup>79a</sup> or K17E, FRT2A/OvoD1, FRT2A were subjected to a heatshock-regime during the larval stages to generate mosaic germline in order to give rise to *rhea* mutant oocytes. Virgins were then crossed to *rhea*<sup>79a</sup> or *rhea*<sup>K17E</sup>/TM6b, *dfd*-GMR- *nvYFP* males. Embryos without the fluorescent balancer were selected for analyses. For all FRAP experiments ubi-talinGFP-WT and ubi-talinGFP-K17E constructs were heterozygous and expressed in a *w*<sup>1118</sup> background. In the case where UAS-driven transgenes were utilized, comparable controls were taken from flies expressing the UAS-transgene, but without the Gal4 driver. Rap1 DN and CA (Ellis et al., 2013) were driven in the muscles using the *mef2*-GAL4 driver.

### **Confocal immunofluorescence imaging and image analysis**

Embryos were fixed and stained according to standard protocols Tanentzapf and Brown, 2006. Antibodies used were against the following proteins: MHC (mouse, 1:200; Dan Kiehart, Duke University, Durham, NC), PINCH (rabbit, 1:1000; Mary Beckerle, Huntsman Cancer Institute, UT), Talin (rabbit, 1:500),  $\alpha$ PS2 (rat, 1:100; 7A10), paxillin (rabbit, 1:1000) (Yagi et al., 2001), tigrin (mouse, 1:500; Liselotte Fessler, UCLA, CA), PINCH (rabbit, 1:1000; Mary Beckerle, University of Utah) and GFP (rabbit, 1:1000; A6455, Invitrogen). Fluorescently-conjugated Alexa-Fluor-488, Cy3 and Cy5 secondary antibodies were used at 1:400 dilution (Molecular Probes). Images were collected using an Olympus FV1000 inverted confocal microscope. For all micrographs of whole embryos, or of MTJs, z- stacks were assembled from 8-12 0.5 $\mu$ m confocal sections. Statistically significant differences were assessed by the two-tailed Student's t-tests in all cases, except when we sought to compare between multiple constructs, where one-way ANOVA was used. Statistical analysis was carried out using Prism4 software (GraphPad, La Jolla, CA). For intensity traces across MTJs, the ImageJ plot profile tool was used to determine the average signal intensity across the boxed area indicated on the images. Intensity curves were obtained from unprocessed grey-scale images so that first the peak intensity of each channel across the area of interest was set as 100%. Each curve was then normalized to the average intensity measured outside of the MTJ.

### **FRAP**

Stage 17 embryos were collected and prepared for FRAP as described previously (Yuan et al., 2010). Briefly, embryos were collected from grape juice plates, dechorinated in 50% bleach for 4 minutes, washed with PBS and mounted onto glass slides in PBS. Photo-bleaching was performed using a 473 nm laser at 5% power with the Tornado scanning tool (Olympus) for 2 seconds at 100 mseconds per pixel. Fluorescence recovery was recorded over 5 minutes at 1 frame every 4 seconds. To control muscle twitching in and out of focus, multiple regions of interest (ROIs) were selected in non-photobleached regions; only samples for which intensities within control ROIs remained steady throughout the FRAP experiment were used. The mobile fraction and statistical tests were performed using Prism 5 software.

### **Western blot analysis and qPCR**

For the quantitative real-time PCR (qPCR) total RNA was isolated from whole flies using TRIzol. A total of 0.5  $\mu$ g total RNA was converted into cDNA using the qScript cDNA Synthesis Kit (Quanta Biosciences). Subsequently, qPCR was performed using iQ SYBR Green Supermix (BIORAD). Talin mRNA levels was averaged between three independent experiments performed four times and normalized to  $\beta$ -tubulin expression. Primers used for Talin were located 3' to the K17E mutation and were as follow GCCAGAACAATACTTTGGGTCG and AACTGGGCATTTTCGCTGGAA.  $\beta$ tubulin expression was determined using the primer pair ATCATCACACACGGACAGGA and GAGCTGGATGATGGGGAGTA. For western blot analysis, protein samples were homogenized in 50mM Tris, 1mM EDTA, 150mM NaCl, 0.5% Triton and EDTA-free complete protease inhibitor cocktail (Roche) and cleared by centrifugation at 13,000 rpm for 30 min at 4°C. After the addition of SDS sample buffer, samples were heated for 5 minutes at 100°C and were resolved using a 7% gel. Primary antibody used: 1:500 mouse anti-talin (E16B, DHSB) and 1:500  $\beta$ -tubulin (E7, DHSB). Secondary antibody used: 1:3000 anti-mouse-HRP (Biorad). Chemiluminescent substrate (Clarity Western ECL Biorad) was

applied via manufacturer instruction and blots were exposed to x-ray film. Triplicate samples were quantified after background subtraction and normalization to  $\beta$ -tubulin bands levels.

### **NMR**

cDNA encoding fly talin residues 1-87 (F0) was synthesized by PCR using a fly talin1 cDNA as template, cloned into the expression vector pet-151, and expressed in *E.coli* BL21 STAR (DE3) cultured in 2xM9 minimal media for preparation of isotopically labelled samples for NMR. Recombinant His-tagged talin polypeptides were purified by nickel-affinity chromatography following standard protocol. The His-tag was removed by cleavage with AcTEV protease (Invitrogen), and the proteins further purified by anion-exchange. Rap1 isoform Rap1b (residues 1-166) cloned into pTAC vector was expressed in *E.coli* strain CK600K. Cultures were grown at 37°C to OD<sub>595</sub> of 0.8 when they were induced with 200  $\mu$ M IPTG and then cultured at 18°C overnight. Protein was purified by ion exchange, followed by gel filtration.

NMR spectra were measured at 298K using a Bruker AVANCE DRX 600 spectrometer equipped with CryoProbe. NMR spectra were obtained using a Bruker AVANCE III 600 MHz spectrometer equipped with CryoProbe. Experiments were performed at 298 K in 20 mM sodium phosphate pH 6.5, 50 mM NaCl, 2 mM DTT with 5% (v/v) <sup>2</sup>H<sub>2</sub>O. Proton chemical shifts were referenced to external DSS. The <sup>15</sup>N and <sup>13</sup>C chemical shifts were referenced indirectly using recommended gyromagnetic ratios (Wishart et al., 1995). Spectra were processed with TopSpin (Bruker) and analysed using ANALYSIS (Vranken et al., 2005).

Ligand binding was evaluated from <sup>1</sup>H,<sup>15</sup>N-HSQC chemical shift changes using 50  $\mu$ M <sup>15</sup>N-labelled F0. Rap1 was added up to a 7 : 1 Rap1:F0 ratio. 3D HNCO, HN(CA)CO, HNCA, HN(CO)CA, HNCACB and HN(CO)CACB experiments were used for the sequential assignment of the backbone NH, N, CO, C $\alpha$  and C $\beta$  resonances as described previously (Skinner et al., 2015). The backbone resonance assignments of fly talin F0 (1-87) have been deposited in the BioMagResBank with the accession number 26884.

## References

- Bellen, H. J., Levis, R. W., Liao, G., He, Y., Carlson, J. W., Tsang, G., Evans-Holm, M., Hiesinger, P. R., Schulze, K. L., Rubin, G. M., et al.** (2004). The BDGP gene disruption project: single transposon insertions associated with 40% of *Drosophila* genes. *Genetics* **167**, 761–81.
- Boettner, B. and Aelst, L. Van** (2009). Control of cell adhesion dynamics by Rap1 signaling. *Curr. Opin. Cell Biol.* **21**, 684–93.
- Bos, J. L., Bruyn, K. de, Enserink, J., Kuiperij, B., Rangarajan, S., Rehmann, H., Riedl, J., Rooij, J. de, Mansfeld, F. van and Zwartkruis, F.** (2003). The role of Rap1 in integrin-mediated cell adhesion. *Biochem. Soc. Trans.* **31**, 83–6.
- Bouaouina, M., Lad, Y. and Calderwood, D. A.** (2008). The N-terminal domains of talin cooperate with the phosphotyrosine binding-like domain to activate beta1 and beta3 integrins. *J. Biol. Chem.* **283**, 6118–25.
- Brown, N. H., Gregory, S. L., Rickoll, W. L., Fessler, L. I., Prout, M., White, R. A. and Fristrom, J. W.** (2002). Talin is essential for integrin function in *Drosophila*. *Dev. Cell* **3**, 569–79.
- Calderwood, D. A., Zent, R., Grant, R., Rees, D. J., Hynes, R. O. and Ginsberg, M. H.** (1999). The Talin head domain binds to integrin beta subunit cytoplasmic tails and regulates integrin activation. *J. Biol. Chem.* **274**, 28071–4.
- Calderwood, D. A., Campbell, I. D. and Critchley, D. R.** (2013). Talins and kindlins: partners in integrin-mediated adhesion. *Nat. Rev. Mol. Cell Biol.* **14**, 503–17.
- Choi, W., Harris, N.J., Sumigray, K.D., and Peifer M.** (2013). Rap1 and Canoe/afadin are essential for establishment of apical–basal polarity in the *Drosophila* embryo. *MBoC.* **24**, 883–1093.
- Chou, T. B. and Perrimon, N.** (1996). The autosomal FLP-DFS technique for generating germline mosaics in *Drosophila melanogaster*. *Genetics* **144**, 1673–9.
- Clark, K. A., McGrail, M. and Beckerle, M. C.** (2003). Analysis of PINCH function in *Drosophila* demonstrates its requirement in integrin-dependent cellular processes. *Development* **130**, 2611–21.
- Costa, P. and Parsons, M.** (2010). New insights into the dynamics of cell adhesions. *Int Rev Cell Mol Biol* **283**, 57–91.
- Daley, W. P. and Yamada, K. M.** (2013). ECM-modulated cellular dynamics as a driving force for tissue morphogenesis. *Curr. Opin. Genet. Dev.* **23**, 408–14.

**Ellis, S. J., Pines, M., Fairchild, M. J. and Tanentzapf, G.** (2011). In vivo functional analysis reveals specific roles for the integrin-binding sites of talin. *J. Cell. Sci.* **124**, 1844–56.

**Ellis, S. J., Goult, B. T., Fairchild, M. J., Harris, N. J., Long, J., Lobo, P., Czerniecki, S., Petegem, F. Van, Schöck, F., Peifer, M., et al.** (2013). Talin autoinhibition is required for morphogenesis. *Curr. Biol.* **23**, 1825–33.

**Ellis, S. J., Lostchuck, E., Goult, B. T., Bouaouina, M., Fairchild, M. J., López-Ceballos, P., Calderwood, D. A. and Tanentzapf, G.** (2014). The talin head domain reinforces integrin-mediated adhesion by promoting adhesion complex stability and clustering. *PLoS Genet.* **10**, e1004756.

**Franco-Cea, A., Ellis, S. J., Fairchild, M. J., Yuan, L., Cheung, T. Y. and Tanentzapf, G.** (2010). Distinct developmental roles for direct and indirect talin-mediated linkage to actin. *Dev. Biol.* **345**, 64–77.

**Giannone, G., Jiang, G., Sutton, D. H., Critchley, D. R. and Sheetz, M. P.** (2003). Talin1 is critical for force-dependent reinforcement of initial integrin-cytoskeleton bonds but not tyrosine kinase activation. *J. Cell Biol.* **163**, 409–19.

**Goult, B. T., Bate, N., Anthis, N. J., Wegener, K. L., Gingras, A. R., Patel, B., Barsukov, I. L., Campbell, I. D., Roberts, G. C. and Critchley, D. R.** (2009). The structure of an interdomain complex that regulates talin activity. *J. Biol. Chem.* **284**, 15097–106.

**Goult, B. T., Bouaouina, M., Elliott, P. R., Bate, N., Patel, B., Gingras, A. R., Grossmann, J. G., Roberts, G. C., Calderwood, D. A., Critchley, D. R., et al.** (2010). Structure of a double ubiquitin-like domain in the talin head: a role in integrin activation. *EMBO J.* **29**, 1069–80.

**Gratz, S. J., Ukken, F. P., Rubinstein, C. D., Thiede, G., Donohue, L. K., Cummings, A. M. and O'Connor-Giles, K. M.** (2014). Highly specific and efficient CRISPR/Cas9-catalyzed homology-directed repair in *Drosophila*. *Genetics* **196**, 961–71.

**Han, J., Lim, C. J., Watanabe, N., Soriani, A., Ratnikov, B., Calderwood, D. A., Puzon-McLaughlin, W., Lafuente, E. M., Boussiotis, V. A., Shattil, S. J., et al.** (2006). Reconstructing and deconstructing agonist-induced activation of integrin  $\alpha$ 5 $\beta$ 3. *Curr. Biol.* **16**, 1796–806.

**Huelsmann, S., Hepper, C., Marchese, D., Knoll, C., and Reuter R.** (2006). The PDZ-GEF Dizzy regulates cell shape of migrating macrophages via Rap1 and integrins in the *Drosophila* embryo. *Development.* **133**, 2915-2924.

**Klapholz, B. and Brown, N. H.** (2017). Talin - the master of integrin adhesions. *J. Cell. Sci.* **130**, 2435–2446.

**Lagarrigue, F., Gingras, A.R., Paul, D.S., Valadez, A.J., Cuevas, M.N., Sun, H., Lopez-Rameriz, M.A., Goult, B.T., Shattil, S.J., Bergmeier, W., and Ginsberg, M.H.** (2018). Rap1 binding to the talin1 Fo domain makes a minimal contribution to murine platelet GPIIb-II activation. *Blood Adv.* **18**, 2358-2368.

**Lee, H.-S. S., Lim, C. J., Puzon-McLaughlin, W., Shattil, S. J. and Ginsberg, M. H.** (2009). RIAM activates integrins by linking talin to ras GTPase membrane-targeting sequences. *J. Biol. Chem.* **284**, 5119–27.

**Leptin, M., Bogaert, T., Lehmann, R. and Wilcox, M.** (1989). The function of PS integrins during *Drosophila* embryogenesis. *Cell* **56**, 401–8.

**Narasimha, M. and Brown, N. H.** (2004). Novel functions for integrins in epithelial morphogenesis. *Curr. Biol.* **14**, 381–5.

**Paul, N. R., Jacquemet, G. and Caswell, P. T.** (2015). Endocytic Trafficking of Integrins in Cell Migration. *Curr. Biol.* **25**, R1092–105.

**Plak, K., Pots, H., Haastert, P. J. Van and Kortholt, A.** (2016). Direct Interaction between TalinB and Rap1 is necessary for adhesion of *Dictyostelium* cells. *BMC Cell Biol.* **17**, 1.

**Schöck, F. and Perrimon, N.** (2003). Retraction of the *Drosophila* germ band requires cell-matrix interaction. *Genes Dev.* **17**, 597–602.

**Schweitzer, R., Zelzer, E. and Volk, T.** (2010). Connecting muscles to tendons: tendons and musculoskeletal development in flies and vertebrates. *Development* **137**, 2807–17.

**Shattil, S. J., Kim, C. and Ginsberg, M. H.** (2010). The final steps of integrin activation: the end game. *Nat. Rev. Mol. Cell Biol.* **11**, 288–300.

**Shirinian, M., Grabbe, C., Popoivc, M., Varshney, G., Hugosson, F., Bos, H., Rehmann, H., and Palmer R.H.** (2010). The Rap1 guanine nucleotide exchange factor C3G Is required for preservation of larval muscle integrity in *Drosophila melanogaster*. *Plos One.* **3**, e9403.

**Skinner, S. P., Goult, B. T., Fogh, R. H., Boucher, W., Stevens, T. J., Laue, E. D. and Vuister, G. W.** (2015). Structure calculation, refinement and validation using CcpNmr Analysis. *Acta Crystallogr. D Biol. Crystallogr.* **71**, 154–61.

**Stritt, S., Wolf, K., Lorenz, V., Vögtle, T., Gupta, S., Bösl, M. R. and Nieswandt, B.** (2015). Rap1-GTP-interacting adaptor molecule (RIAM) is dispensable for platelet integrin activation and function in mice. *Blood* **125**, 219–22.

**Tadokoro, S., Shattil, S. J., Eto, K., Tai, V., Liddington, R. C., Pereda, J. M. de, Ginsberg, M. H. and Calderwood, D. A.** (2003). Talin binding to integrin beta tails: a final common step in integrin activation. *Science* **302**, 103–6.

- Tanentzapf, G. and Brown, N. H.** (2006). An interaction between integrin and the talin FERM domain mediates integrin activation but not linkage to the cytoskeleton. *Nat. Cell Biol.* **8**, 601–6.
- Tanentzapf, G., Martin-Bermudo, M. D., Hicks, M. S. and Brown, N. H.** (2006). Multiple factors contribute to integrin-talin interactions in vivo. *J. Cell. Sci.* **119**, 1632–44.
- Torgler, C. N., Narasimha, M., Knox, A. L., Zervas, C. G., Vernon, M. C. and Brown, N. H.** (2004). Tensin stabilizes integrin adhesive contacts in *Drosophila*. *Dev. Cell* **6**, 357–69.
- Vranken, W. F., Boucher, W., Stevens, T. J., Fogh, R. H., Pajon, A., Llinas, M., Ulrich, E. L., Markley, J. L., Ionides, J. and Laue, E. D.** (2005). The CCPN data model for NMR spectroscopy: development of a software pipeline. *Proteins* **59**, 687–96.
- Wegener, K. L., Partridge, A. W., Han, J., Pickford, A. R., Liddington, R. C., Ginsberg, M. H. and Campbell, I. D.** (2007). Structural basis of integrin activation by talin. *Cell* **128**, 171–82.
- Wehrle-Haller, B.** (2012). Assembly and disassembly of cell matrix adhesions. *Curr. Opin. Cell Biol.* **24**, 569–81.
- Wishart, D. S., Bigam, C. G., Yao, J., Abildgaard, F., Dyson, H. J., Oldfield, E., Markley, J. L. and Sykes, B. D.** (1995). <sup>1</sup>H, <sup>13</sup>C and <sup>15</sup>N chemical shift referencing in biomolecular NMR. *J. Biomol. NMR* **6**, 135–40.
- Wolfenson, H., Lavelin, I. and Geiger, B.** (2013). Dynamic regulation of the structure and functions of integrin adhesions. *Dev. Cell* **24**, 447–58.
- Yagi, R., Ishimaru, S., Yano, H., Gaul, U., Hanafusa, H. and Sabe, H.** (2001). A novel muscle LIM-only protein is generated from the paxillin gene locus in *Drosophila*. *EMBO Rep.* **2**, 814–20.
- Yang, J., Zhu, L., Zhang, H., Hirbawi, J., Fukuda, K., Dwivedi, P., Liu, J., Byzova, T., Plow, E. F., Wu, J., et al.** (2014). Conformational activation of talin by RIAM triggers integrin-mediated cell adhesion. *Nat Commun* **5**, 5880.
- Yuan, L., Fairchild, M. J., Perkins, A. D. and Tanentzapf, G.** (2010). Analysis of integrin turnover in fly myotendinous junctions. *J. Cell. Sci.* **123**, 939–46.
- Zervas, C. G., Gregory, S. L. and Brown, N. H.** (2001). *Drosophila* integrin-linked kinase is required at sites of integrin adhesion to link the cytoskeleton to the plasma membrane. *J. Cell Biol.* **152**, 1007–18.
- Zhu, L., Yang, J., Bromberger, T., Holly, A., Lu, F., Liu, H., Sun, K., Klapproth, S., Hirbawi, J., Byzova, T. V., et al.** (2017). Structure of Rap1b bound to talin reveals a pathway for triggering integrin activation. *Nat Commun* **8**, 1744.

## Figures

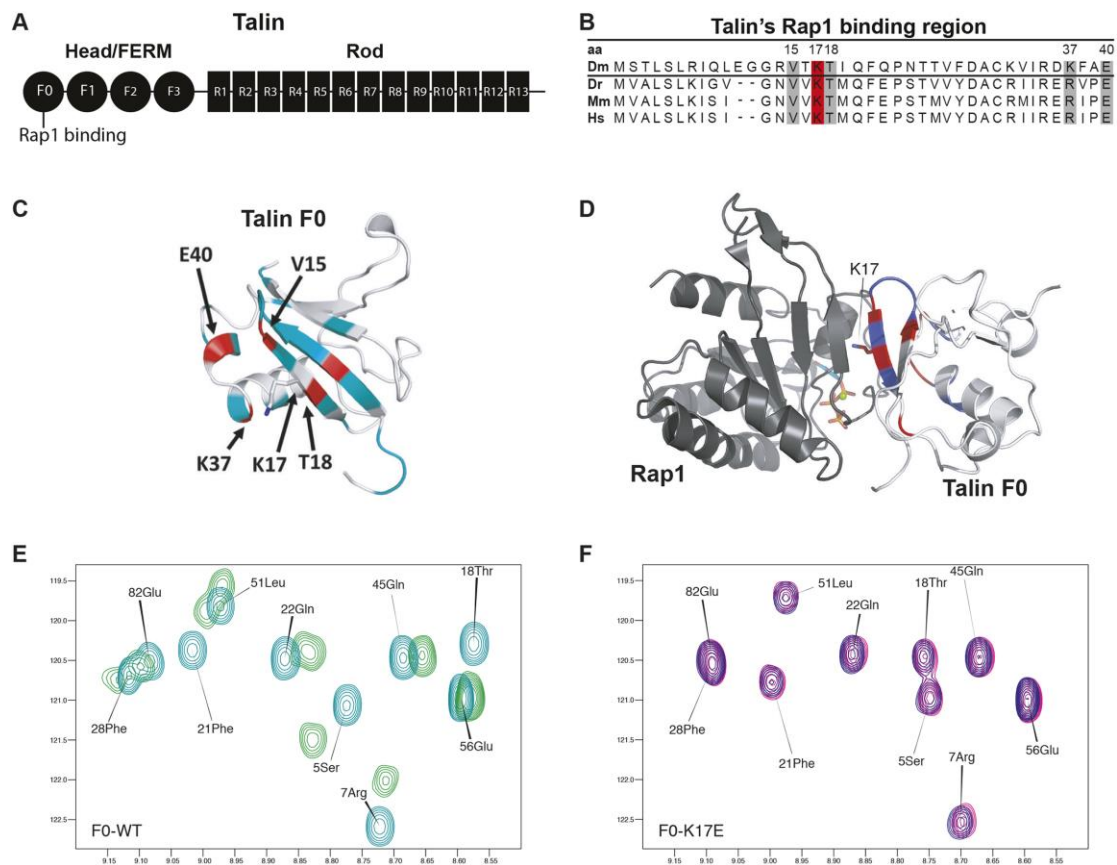


### Figure 1. Biochemical and structural characterization of the Rhea-F0 Rap1 interaction.

(A) Schematic representation of Talin's FERM and rod domains and the location of the Rap1 binding region in the F0 domain of the Talin head. (B) Sequence alignment of the Rap1 binding region from fly (Dm Talin), zebrafish (Dr Talin1), mouse (Mm Talin1) and human (Hs Talin1) talins. Amino acid numbering is based on Dm Talin. Shading (grey and red) indicates positively charged residues important for Rap1 binding. Red shading indicates the position of K17, the residue mutated in this study. (C) Mapping of the Rap1 binding site on Rhea-F0. Conserved residues shown in (B) are marked. (D) Structural model of the Talin-F0:Rap1 interaction. Weighted chemical shift differences, determined as described previously (Goult et al., 2009), are shown on ribbon representations of the F0:Rap1b structure; peaks that broaden are shown in blue, shifts > 0.13 ppm are in red. (E-F)  $^1\text{H},^{15}\text{N}$  HSQC spectra of 50  $\mu\text{M}$   $^{15}\text{N}$ -labeled rhea F0 (residues 1-87) in the absence or presence of Rap1b; (F) wildtype F0 alone (teal) and with Rap1 (green) (G) K17E F0 alone (pink) and with Rap1 (purple).

Kdv

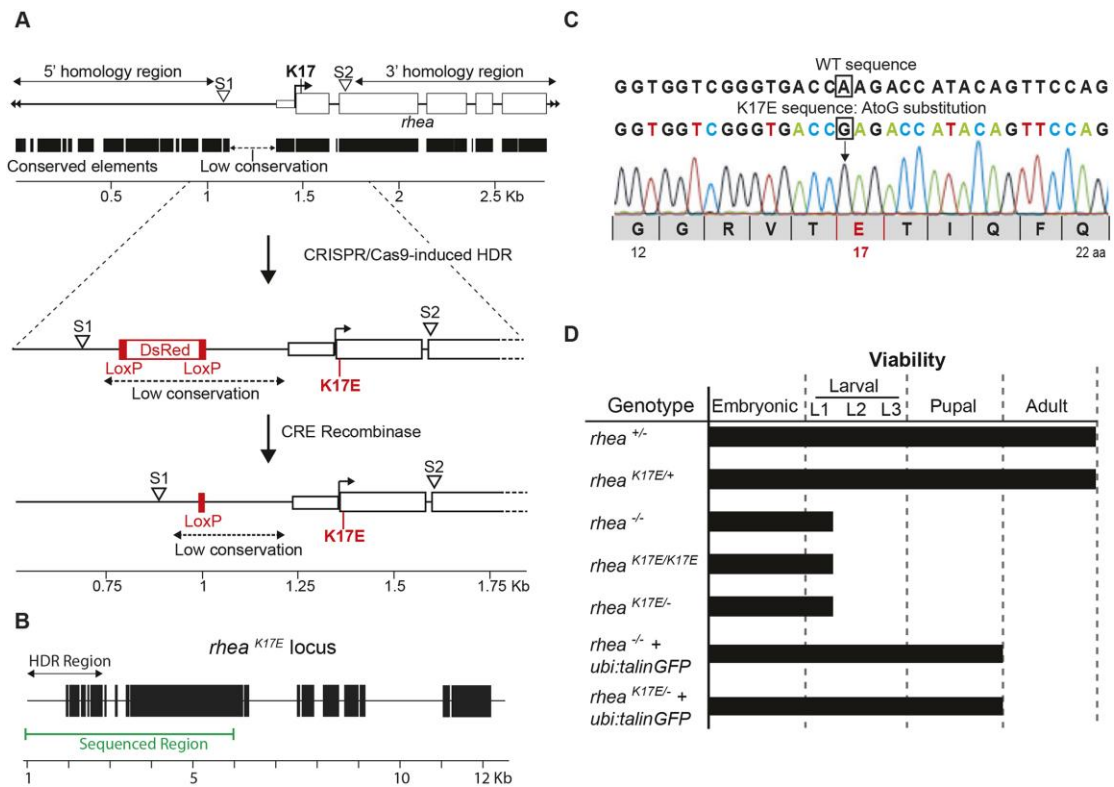


## Figure 2. Generation of the K17E Talin mutant

CRISPR strategy to introduce the K17E substitution in *rhea* locus. S1 and S2 represent the cut sites targeted by Cas9, red elements represent inserted modifications (see materials and methods). (B) Schematic of the *rhea* locus, sequenced region shown in green. (C) Representative electropherogram of K17E mutant flies sequencing. (D) K17E viability in diverse genetic back- ground ( $n > 100$  per genotype).

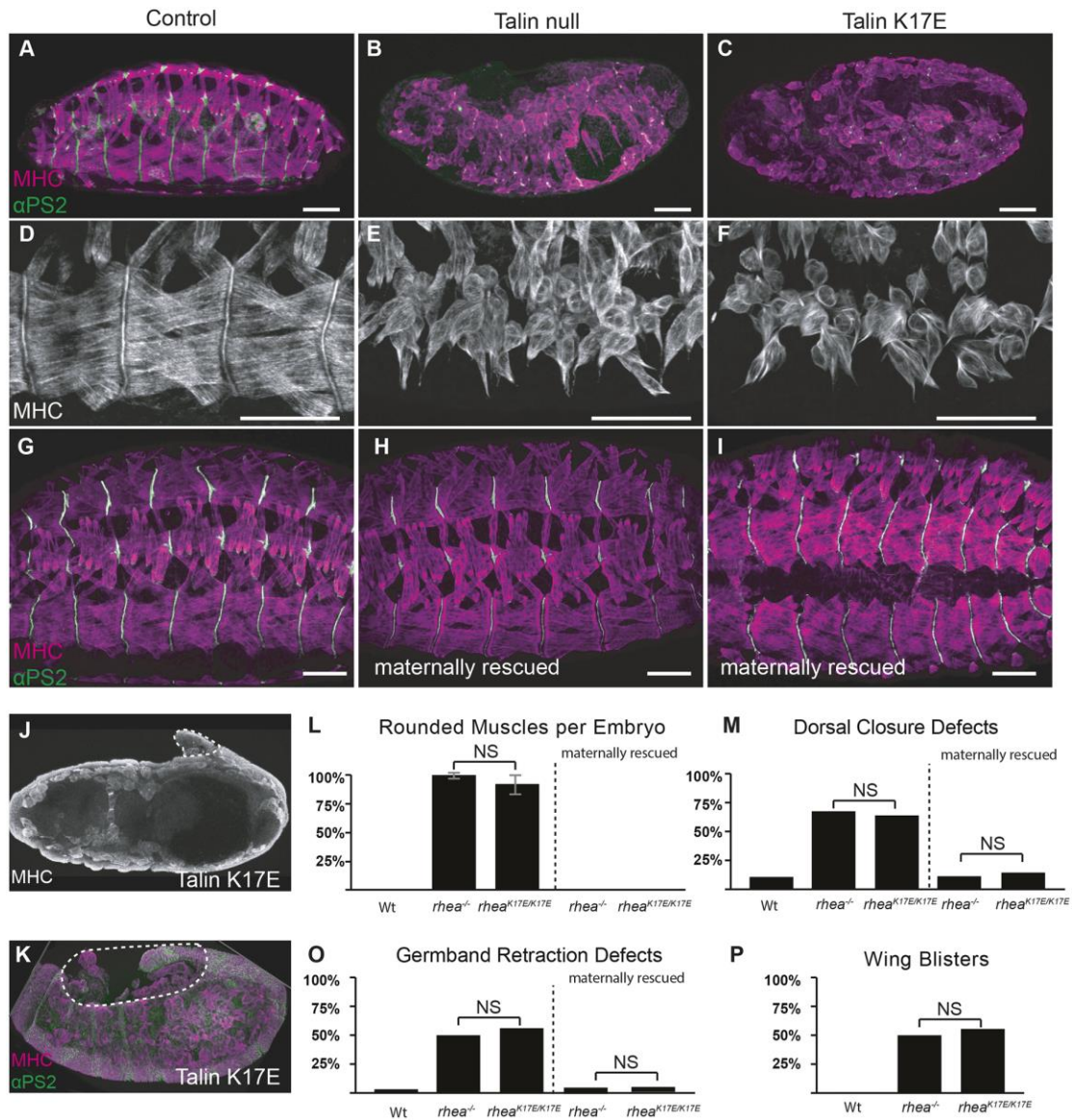


### Figure 3. Rap1 binding is strictly required for Talin function.

(A-K) Confocal images of whole-mount embryos stage 17. (A-C, G-I) Whole embryo view stained for Integrin in green and a muscle cytoskeleton marker Myosin Heavy Chain (MHC) in magenta, (D-F) Representative muscles stained with MHC in hemisegments A2-A6. Control (A and D), Talin-null (B and E) and K17E embryos (C and F). Control embryo (G), Talin-null (H) and K17E (I) embryos with maternal contribution (see materials and methods). (J) Representative germband retraction defect giving the embryo a characteristic ‘tail up’ phenotype highlighted by the dotted line in a K17E embryo stained for MHC. (K) Representative dorsal closure defect (dotted line highlights persistent dorsal hole) in a K17E embryo stained for Integrin (green) and MHC (magenta). (L-P) Penetrance of muscle (L), dorsal closure (M), germband retraction (O) and wing (P) defects in embryos of the indicated genotypes. Scale Bars = 50  $\mu$ m. Error bars represent s.e.m. (\*  $P < 0.05$ ), NS=no significance ( $n > 30$  for each genotype)).

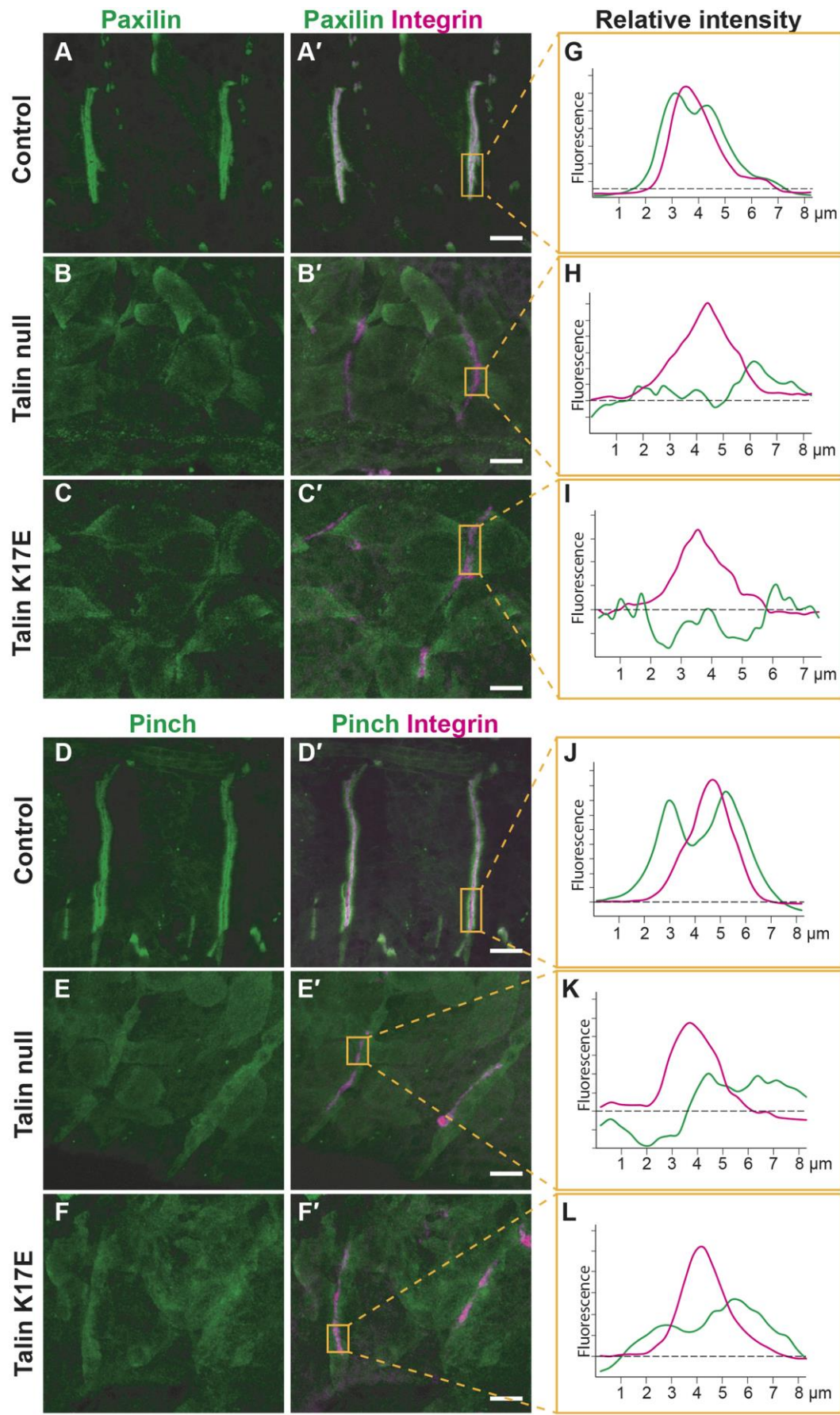


**Figure 4. IAC components recruitment to MTJs is disrupted in K17E mutants.** (A-F') Confocal z-stacks of MTJs in stage 17 Talin-null embryos stained for PS2 Integrin (magenta A-F') and IAC components: Paxillin (green, A-C') and Pinch (green, D-F'). (G-L) Average intensity profiles of PS2 Integrin (magenta, G-L), Paxillin (green, G-I) and Pinch (green, J-L) across the widths of the boxed areas indicated in the corresponding images. Dotted line indicates average intensity outside of the MTJ. Scale Bars = 10  $\mu$ m.

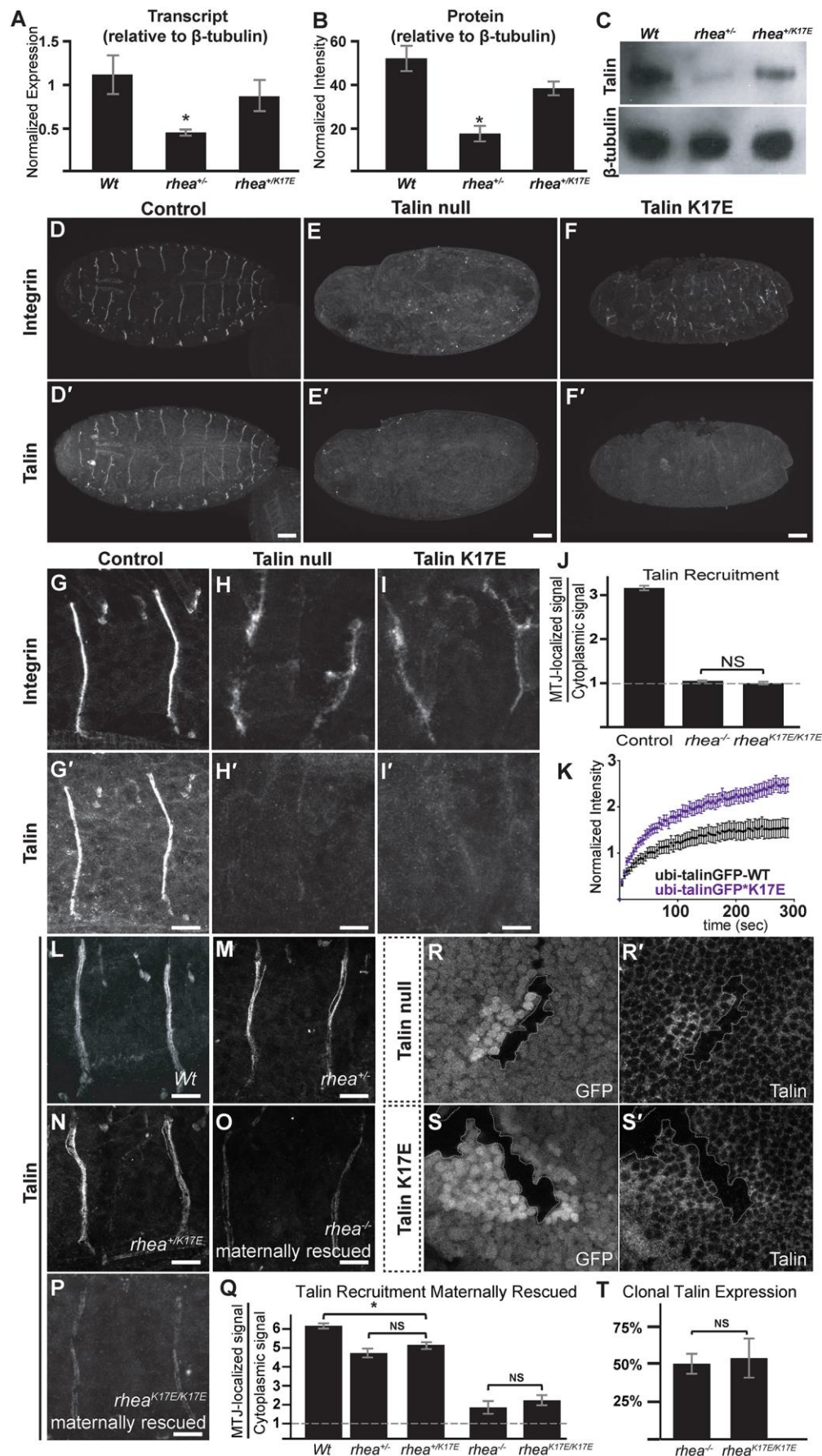


**Figure 5. Talin K17E recruitment.**

Relative Talin expression levels determined via qRT-PCR and (B,C) western blot analysis of Wt, *rhea*<sup>+/-</sup> and *rhea*<sup>+/K17E</sup> heterozygote flies. (D-F) Representative confocal images of whole-mount stage 17 embryos stained for Integrin  $\alpha$ PS2 (D-F) or Talin (D'-F'). (G-J) Talin (G,H and I) and Integrin (G', H' and I') recruitment at MTJs in control (G and G'), Talin null (H and H') and K17E embryos (I and I'). (J) Relative localization of Talin to MTJ's. (K) Average recovery intensity of talin GFP (black) and talin K17E GFP (purple) over time from bleached embryonic MTJs presented with 95% confidence intervals (see materials and methods). (L-Q) Zygotic and maternal Talin expression in control (L), Talin heterozygote (M), K17E heterozygote (N), as well as Talin null (O) and K17E (P) both maternally rescued. (Q) Relative localization of zygotic and maternal Talin to MTJ's. (R-T) Clonal analysis of Talin mutants in the wing disc. Talin null clones (R') and K17E clones (S') are located by the absence of GFP (R and S). (T) Staining intensity inside the clone relative to average outside of the clone intensity. Scale Bars = 50  $\mu$ m for D-F', 10  $\mu$ m for G-O. Relative localization was determined by averaging results from 3 MTJs per larva (n>10 per genotypes or clones). Error bars for (A, J, K, Q and T) represent s.e.m. and SD for (B). (\* P<0.05), NS=no significance.

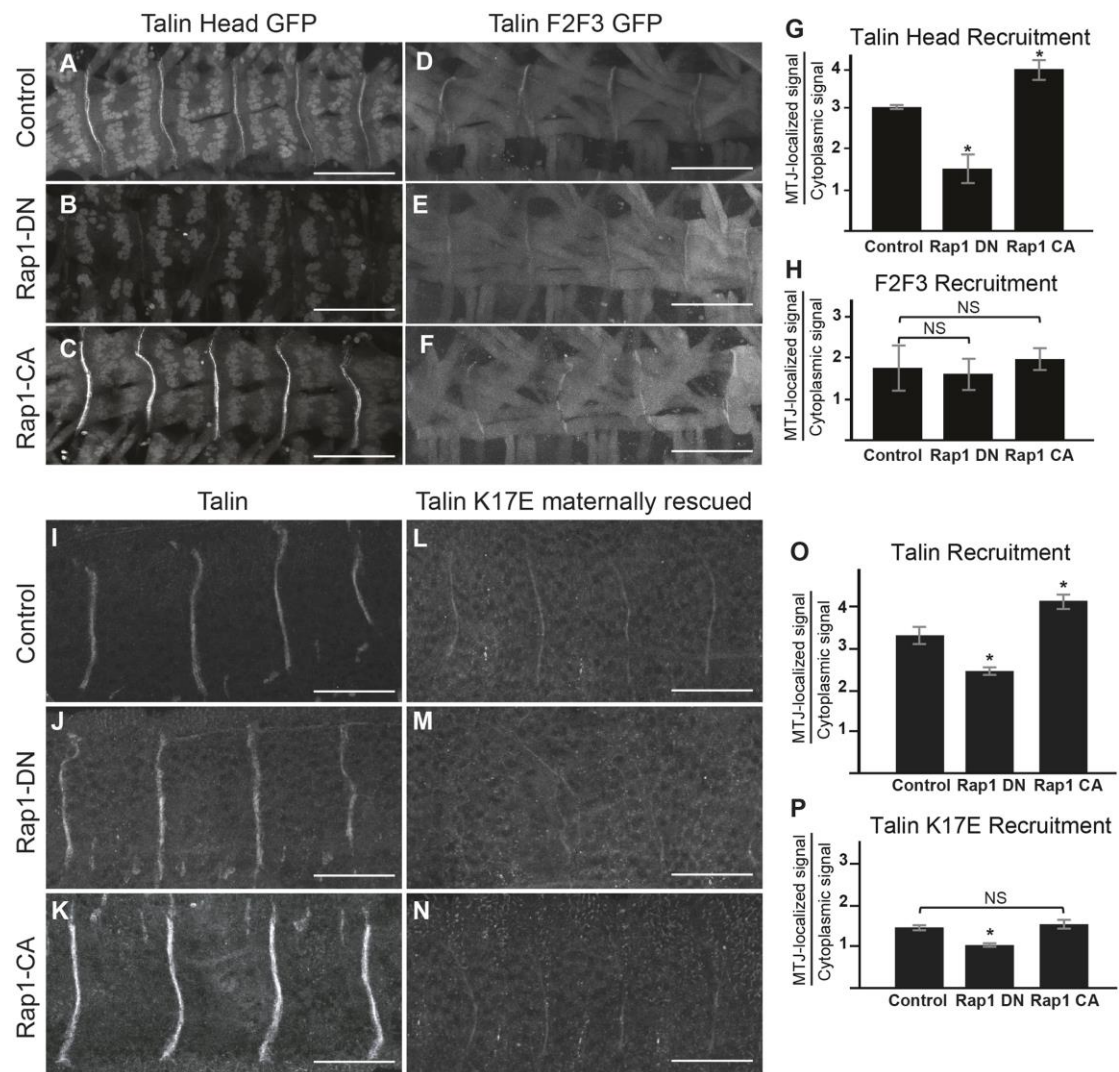
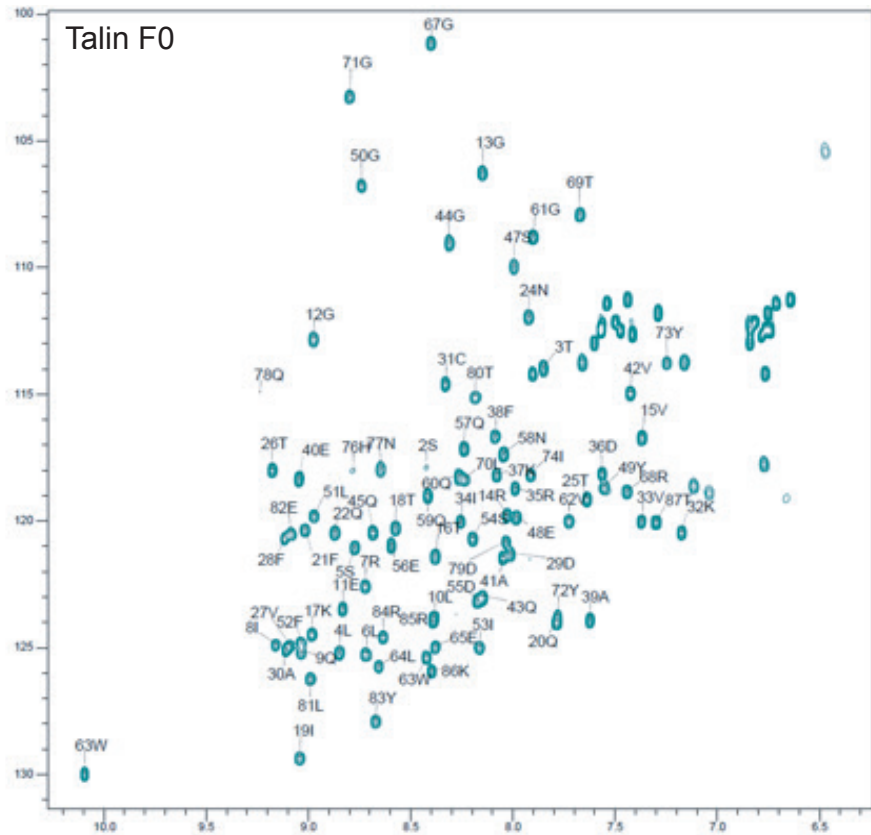


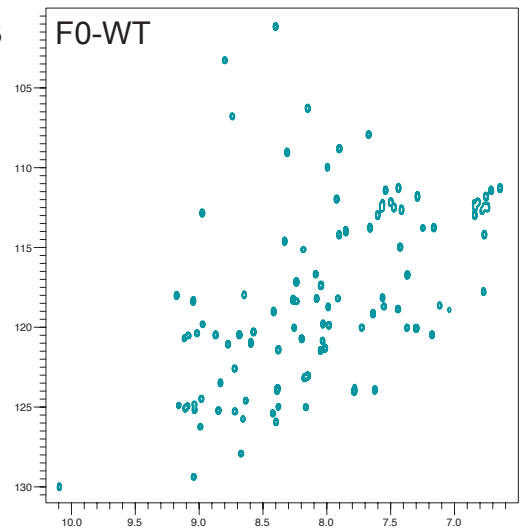
**Figure 6. Rap1 modulation of Talin recruitment requires K17.**

(A-F) Muscles in wildtype, live, stage 17 embryos ubiquitously expressing the GFP-tagged Talin head (Talin Head GFP; A-C) and version deleting the most N-terminal region which includes the Rap1 binding domain (Talin F2F3-GFP; D-F). Talin head or F2F3 recruitment to the MTJs was assessed in control embryos (A and D) and embryos either expressing a dominant negative form of Rap1 (Rap1-DN, B and E) or a constitutively active form (Rap1-CA, C and F). (G and H) Relative localization of Talin head-GFP (G) and Talin F2F3-GFP (H) to MTJs in control, Rap1- DN and Rap1-CA expressing embryos. (I-K) Zygotic and maternal Talin expression in control (K), Rap1-DN (J) or Rap1-CA (K) expressing embryos. (L-N) Zygotic and maternal Talin expression in K17E control (L), Rap1-DN (M) or Rap1-CA (N) expressing embryos. (O) Relative localization of zygotic and maternal Talin to MTJ's in control, Rap1-DN and Rap1-CA expressing embryos. (P) Relative localization of zygotic and maternal Talin to MTJ's in control, Rap1-DN and Rap1-CA expressing K17E embryos. Scale Bars = 50  $\mu$ m. Relative localization was determined by averaging results from 3 MTJs per larva ( $n > 10$  per genotypes). Error bars represent s.e.m. (\*  $P < 0.05$ ), NS=no significance.

A



B



C

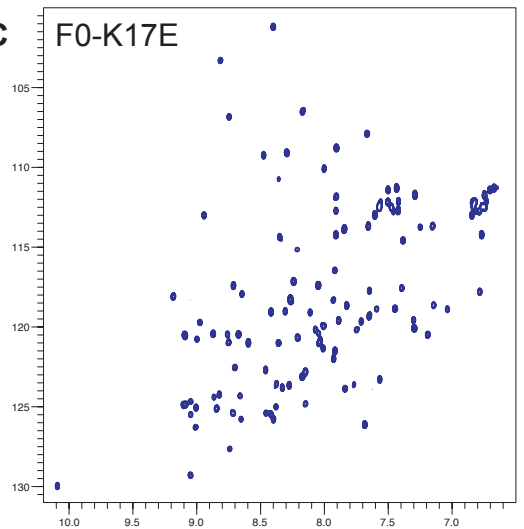


**Figure S1.**

(A) Assigned  $^1\text{H}$ ,  $^{15}\text{N}$  HSQC spectrum of fly Talin F0 (residues 1-87). (B-C)  $^1\text{H}$ ,  $^{15}\text{N}$  HSQC spectra of talin F0 (B) wildtype and (C) K17E.

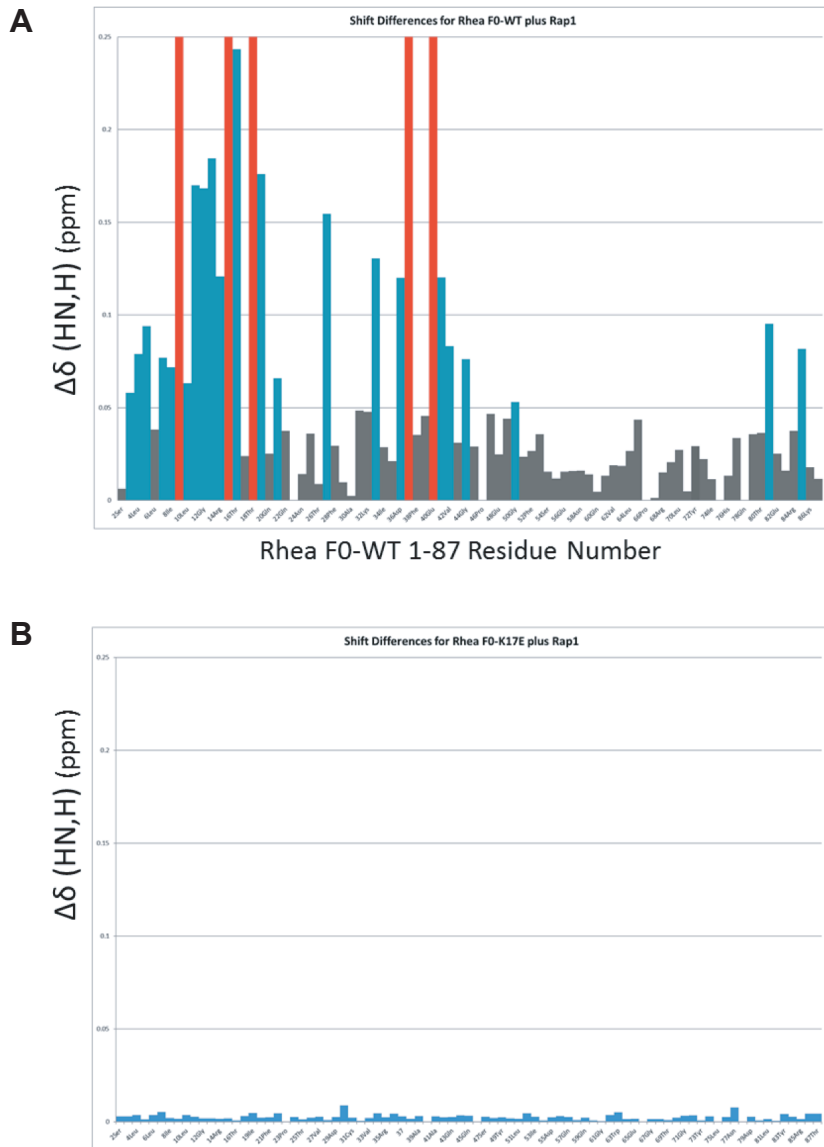


**Figure S2.**

(A-B) Weighted shift map obtained from the  $^1\text{H}$ ,  $^{15}\text{N}$  HSQC spectra of the talin F0 domain with the addition of Rap1b. (A) Wildtype F0 and (B) K17E F0.